Evaluation of a Low-cost Camera for Agricultural Applications

Abdon Francisco Aureliano Netto[1*], Rodrigo Nogueira Martins[2],
Guilherme Silverio Aquino de Souza[3], Fernando Ferreira Lima dos Santos[2]
and Jorge Tadeu Fim Rosas[2]

[1]*Department of Electrical Engineering, Federal University of São João Del Rei, Brazil.*
[2]*Department of Agricultural Engineering, Federal University of Viçosa, Brazil.*
[3]*Department of Forestry, Federal University of Viçosa, Brazil.*

Authors' contributions

This work was carried out in collaboration among all authors. All authors read and approved the final manuscript.

Original Research Article

ABSTRACT

This study aimed to modify a webcam by replacing its near-infrared (NIR) blocking filter to a low-cost red, green and blue (RGB) filter for obtaining NIR images and to evaluate its performance in two agricultural applications. First, the sensitivity of the webcam to differentiate normalized difference vegetation index (NDVI) levels through five nitrogen (N) doses applied to the Batatais grass (*Paspalum notatum* Flugge) was verified. Second, images from maize crops were processed using different vegetation indices, and thresholding methods with the aim of determining the best method for segmenting crop canopy from the soil. Results showed that the webcam sensor was capable of detecting the effect of N doses through different NDVI values at 7 and 21 days after N application. In the second application, the use of thresholding methods, such as Otsu, Manual, and Bayes when previously processed by vegetation indices showed satisfactory accuracy (up to 73.3%) in separating the crop canopy from the soil.

_____

*Corresponding author: E-mail: abdonfan@hotmail.com;

1. INTRODUCTION

Recent developments in sensor technologies have made digital cameras more and more efficient and affordable. These systems have been widely used as a versatile remote sensing tool for many applications due to its advantages over film-based aerial photography and satellite imagery [1]. The main advantage of digital photography lies in simplified image processing [2]. Among the advantages of digital photography from these cameras are its relatively low cost, high spatial resolution and near-real-time availability of imagery for visual assessment and image processing.

Digital cameras are fitted with either a charge-coupled device (CCD) sensor or a complementary metal oxide semiconductor (CMOS) sensor that are photoconductive devices. These sensors are sensitive to near-infrared (NIR) wavelengths, however, most of these cameras are fitted with a blocking filter to this wavelength. Thus, typically these images present only the red, green, and blue (RGB) bands, which are sufficient to represent colors in the visible portion of the spectrum (400 – 700 nm), as recognized by the human vision [3]. In most cases, the digital photographs are recorded in joint photographic experts' group (JPEG) or tagged image file format (TIFF), and the RGB channels are obtained through image processing.

The use of images with RGB and NIR bands is very common in agricultural applications, especially for vegetation monitoring. Many vegetation indices, such as the normalized difference vegetation index (NDVI) [4] require spectral information in the NIR and red bands, even though the RGB bands could be sufficient for some applications [5]. Since most consumer-grade cameras only provide RGB bands, NIR filtering techniques can be used to convert an RGB camera into a NIR camera. Moreover, it is possible to replace the blocking filter by a long-pass infrared filter on standard CCD or CMOS sensors for obtaining NIR images [6].

Over the years, numerous systems for collecting images based on cameras or webcams have been developed and modified to obtain NIR information across multiple domains. Most systems included analysis of the nutritional status of agricultural crops [7], disease detection [8], yield estimation [9], and weed identification [10]. In addition, other authors highlight the possibilities of using vegetation indices combined with segmentation techniques and texture analysis for obtaining data of interest, such as crop canopy and soil [11,12]. Furthermore, these cameras can be mounted in a stationary installation [13] or onboard a light aircraft or unmanned aerial vehicle, a deployment which was made possible due to its low weight [14,15].

Given the many possibilities of using images from RGB or modified cameras to access the NIR band, the use of artificial vision systems through image processing has enabled the extraction of information of interest, which proves to be a great tool for application in the agricultural environment. However, there are still factors, such as different ambient lighting conditions, plant shading and complex background that are challenges to the success of using low-cost images for agricultural applications as described in other studies [16,17]. Therefore, in view of the challenge to obtain these images with good quality for solving problems, the present study aimed to modify a webcam to obtaining data from the NIR band and to evaluate its performance over different agricultural applications.

2. MATERIALS AND METHODS

The experiment was conducted at the Federal University of Viçosa, Viçosa Campus in Minas Gerais, which is located among the coordinates: 20° 45' 14 "(S) and 42° 52' 54" (W), 649 meters above sea level. The image acquisition system comprised two C3 Tech model HB 2105 webcams that produced images in JPEG format (640x480 pixels).

In order to obtain NIR images, a modification was carried out in one of the webcams by removing the NIR blocking filter and adding an RGB blocking filter, which was made from the magnetic material of a floppy disk (common diskette) as proposed by Micha et al. [18]. Thus, the unmodified webcam, named in this study as RGB webcam and the modified NIR webcam were tested on two different applications. First, the performance of the webcam's images to differentiate NDVI values according to different N rates was verified. Second, these images were processed for separating the crop canopy from the soil using different thresholding algorithms.

In the first application, a field experiment was carried out using the Batatais grass (*Paspalum notatum* Flugge), where a randomized block design with five treatments and five replications was adopted. Treatments consisted of five nitrogen (N) doses in the form of ammonium sulfate (($NH_4)_2SO_4$), which corresponded to 0, 40, 80, 120 and 160 kg ha^{-1}. Plot dimensions were 1 m × 1 m.

Furthermore, the digital images were captured with both webcams at a height of 3 m from the ground using a ladder, with the webcam being held by one of the authors, and always ensuring that the image was taken to cover the entire area of the experimental plot. Data acquisition was performed twice with images being captured at 7 and 21 days after the N application. All images were geometrically corrected through the projective transformation technique using the Matlab[®] software, where reference points were defined at the boundaries of each plot. Lastly, the NDVI [4] was calculated by Equation 1 for each experimental plot.

$$NDVI = \frac{nir - r}{nir + r} \qquad (1)$$

Where:

nir: near-infrared band; and r: red band.

In addition, the portable chlorophyll meter (SPAD-502, Konica Minolta Sensing, Tokyo, Japan) was used to measure the SPAD index (SI) [19]. Thus, at the 7 and 21 days after N application, 30 readings per plot were taken, where the average of all readings was considered as a result. In this study, the SPAD-502 readings were assumed to be the reference of chlorophyll content for the purpose of validating the sensitivity of the webcams in detecting the effect of N doses over the Batatais grass.

In order to verify the significance of the proposed treatments, the results were submitted to analysis of variance (ANOVA) through the F-test. Lastly, regression models were adjusted to assess treatment effects on the results of the SPAD index readings and NDVI values. All analyses were carried out using the ASSISTAT, version 7.7 free software [20].

In the second application, the RGB images were used for the ability to differentiate crop canopy from soil under different growing conditions. There were 30 images captured for this study

and all of it belonged to maize crops at the *V4* vegetative stage (*four expanded leaves*), which were grown under different soil cover conditions, such as conventional planting system, and no-tillage system with coffee husk and straw residue.

The digital images were captured at a height of 1.5 m from the ground and then stored as 24-bit colour images with resolutions of 640 × 480 pixels saved in RGB colour space in the JPEG format. Then, to discriminate between the object of interest (plant) and background (soil), algorithms were developed using different thresholding methods, such as Otsu [21], Manual threshold selection, and Bayes [22].

Initially, two methods were used to accentuate the green color of plants in RGB images. First, in the absolute green method, the pixel color distance (PCD) value was obtained through the Euclidean distance (ED) calculation using normalized values from the red and green bands of each pixel, as shown in Equation 2 [23].

$$PCD = \sqrt{pixel(r^2) + [pixel(g) - 1]^2} \qquad (2)$$

Where,

r: pixel value from the red band; and g: pixel value from the green band.

Second, the excess green normalized index (ExG) was obtained as it is shown in Equation 3 [24].

$$ExG = \frac{2 \times g - r - b}{r + g + b} \qquad (3)$$

Where,

g: pixel value from the green band; r: pixel value from the red band; and b: pixel value from the blue band.

Subsequently, the Otsu, Manual, and Bayes methods were applied to each image. As a result, all images showed some noise, which was removed by using a median filter with a 3 m × 3 m window size. Moreover, the ground truth segmentation model for comparison of the three algorithms was developed from the K-means method.

Generally, this method can be employed in different areas including image processing, where it can be used as a thresholding method

based on data clustering. This method partitions n pixels into k clusters, where k is an integer value that holds k < n. The k-means algorithm classifies pixels in an image into k number of clusters according to some similarity feature, such as the grey level intensity of pixels, and distance of pixel intensities from centroid pixel intensity [25].

The algorithm is based on six steps:

1. Selection of k clusters (k is a user-defined parameter);
2. Calculation of the number of image pixels N;
3. Selection of k initial pixel intensity centroids µj;
4. Calculation of distances D_{ij} between pixel x_i and each centroid µj as given in Equation 4.

$$D_{ij} = (x_i - \mu_j)^2 \tag{4}$$

Where:

i = 1 ÷ N; and j = 1 ÷ k.

Particular pixel x_i is then classified to cluster c_j to which centroid it has the smallest distance.

5. Recalculation of centroid positions µj as a mean value of all pixel intensities, which belong to cluster cj as shown in Equation 5.

$$\mu_t = \frac{1}{l_j} * \sum_{i=1}^{l_j} x_i \tag{5}$$

Where,

l_j is the number of pixels that belong to cluster c_j.

6. Steps (4) and (5) are repeated until the classification of the image pixels does not change.

In this study, the value of k (number of clusters) was defined as two, where the first represented the crop canopy and second the soil. Then, in order to validate the performance of each thresholding method, the accuracy index, proposed by Coy et al. [26] was computed using Equation 6.

$$Accuracy = 100 \times \frac{A \cap B}{A \cup B} \tag{6}$$

Where:

A: represents the set of pixels in the ground truth image that is marked as crop canopy; and; B: represents the set of pixels in the segmentation that is marked as crop canopy.

This measure of accuracy determines how closely the segmentation matches the ground truth, with 100% indicating an exact match and perfect segmentation. Thus, to verify the significance of the proposed methods, the accuracy means were compared by the Students t-test at a 5% significance level (α <0.05).

3. RESULTS AND DISCUSSION

3.1 Application 1

Average values of the SI and NDVI as a function of the nitrogen doses, as well as its respective coefficient of variation (CV), are shown in Table 1. It can be observed that CV values for NDVI index tended to be higher than to SI values at 7 and 21 days, which may be justified by the low uniformity of the Batatais grass on the study area. Furthermore, the fact that SPAD readings are done by direct contact with the leaf surface might have decreased its CV. In addition, its higher number of readings per plot also contributes to decrease CV values, which is not done in the NDVI calculation, since only one RGB, and NIR images are used per plot to obtain the index.

Table 1. Descriptive statistics of the SI (SPAD index) and NDVI (normalized difference vegetation index) at 7 and 21 days after N application

Time Days	N rates (kg ha⁻¹)					CV
	0	40	80	120	160	(%)
SI (SPAD-502)						
7	40.22	43.17	43.20	44.95	47.00	3.67
21	37.95	44.92	48.12	45.82	46.95	6.55
NDVI (webcam)						
7	0.19	0.23	0.27	0.31	0.33	26.4
21	0.23	0.25	0.26	0.22	0.39	17.9

CV: Coefficient of variation

Even showing sensitivity to the applied N rates, NDVI results from both dates (7 and 21 days) were relatively low, which might be associated with low uniformity of the vegetation, and absence of radiometric calibration. Petach et al. [27] highlights that using a reference panel for standardization or the inclusion of a gray Spectralon (or other diffuse reflectors) panel within the field of view of the webcam would potentially be of value for calibration under changing illumination conditions (e.g. cloudy vs. sunny days). Thus, a radiometric calibration could increase the sensitivity of the webcam, which would result in higher NDVI values and lower weather interference. However, the results obtained here suggest that even without this calibration, the webcam was still capable of detecting differences among treatments.

The regression analyses carried out to access the effect of nitrogen doses on SI and NDVI values at 7 and 21 days after N application showed a linear (7 days) and quadratic (21 days) response for both indices. Moreover, both indices were significant at 1% probability with a coefficient of determination (R^2) of 0.93 (SI, p-value: 0.0001), and 0.98 (NDVI, p-value: 0.008), respectively. In Fig. 1 it is possible to observe the linear increase of the SI and NDVI values as the N doses increases at 7 days after the fertilization.

When observing the SI values at 21 days (Fig. 1), a linear increase in its values is also observed up to the dose of 80 kg ha^{-1} of N. However, from the 120 kg ha^{-1} of N, SI values showed a decrease, which demonstrates a quadratic response to different N doses with a R^2 of 0.8931 (p-value: 0.0068). Similarly, NDVI values showed a linear increase up to 80 kg ha^{-1} of N. Although, when looking at 120 and 160 kg. ha^{-1} N doses, NDVI response showed a high variation for both treatments, which resulted in low correlation (R^2 = 0.67) (p-value: 0.0169). This high variation in the NDVI response is possibly associated with the low uniformity of the grass, as well as to changes in weather and illumination conditions, which might have influenced the visual quality of the images. Even though there was a high variation in response to these treatments, SI and NDVI values at 21 days were also significant at 1%, and 5% probability, respectively.

In general, this quadratic response for both indices at 21 days indicates that, in this range, increasing the nutrient concentration (nitrogen) would not reflect on grass growth, and it represents the plant luxury consumption. According to Baesso et al. [28], luxury consumption is defined as the N storage in the vacuole instead of its participation in the chlorophyll molecule. The same authors also point out that, excessive consumption is not always undesirable since it allows plants to accumulate nutrients when its availability is high. In this case, a gradual release is performed by the plant, when the absorption is insufficient to support its growth.
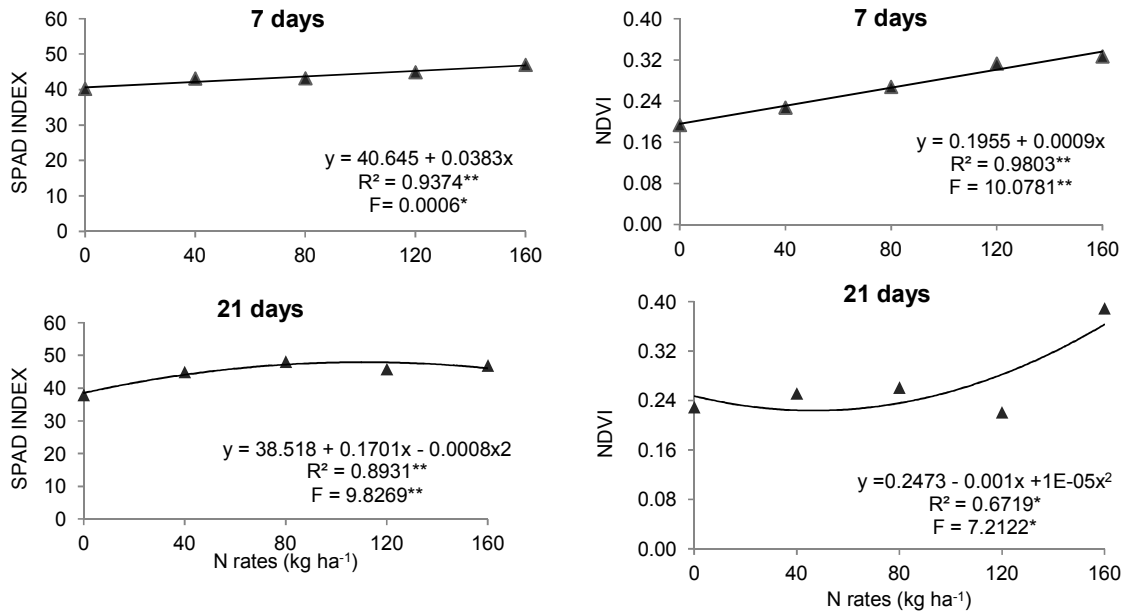

Fig. 1. SPAD index (SI) and NDVI index as a function of topdressing nitrogen doses

Results obtained in this study showed that the webcam sensor evaluated was capable of detecting the effect of N doses over the Batatais grass for both dates, at 7 and 21 days after N application. The SPAD-502 used here as a reference method presented better results, which was expected due to its higher sensitivity and correlation with the leaf chlorophyll content.

Compared to other low-cost, sensor-based methods for monitoring crops phenology, such as radiometric instruments based on LED sensors [29], or light-emitting diodes [30], a clear advantage of using webcams is that it can yield images with good spatial resolution. This enables tracking the phenology of different crops by breaking the image into different regions of interest (e.g., crops and weeds) [27]. On the other hand, there is no doubt that higher-quality spectral imaging could, potentially, be obtained from existing, commercially available multispectral cameras. However, for budget-limited observational and experimental studies, the system proposed here may represent an acceptable compromise, given its low cost and promising performance.

3.2 Application 2

Initially, performance analyses of segmentation algorithms were based on visual analysis by comparing the proposed methods to the reference binary image. Then, the accuracy index (equation 6) was used for comparing each result with that obtained through the K-means. In general, segmentation methods when combined with the ExG index showed higher accuracy results than those methods preceded by the Euclidean distance (ED). Moreover, the highest overall mean accuracy (80.3%) was obtained using the Otsu method preceded by ExG index. On the other hand, the lowest accuracy mean was observed using the Manual method with the ED index (73.3%).

These results corroborate with [31], which observed that images segmented by the Otsu with the ExG index showed 88% accuracy when compared to other indices using RGB bands. In another study [32], these authors when using the Otsu method preceded by different indices, such as ExG, ExR (excess of red), and another index based on the CIE l*a*b color space obtained accuracies of 74%, 77.2%, and 62%, respectively. This demonstrates that the contrast provided by vegetation indices is of great use to highlight the crop canopy from the soil, and could yield in high accuracy segmentation.

When analyzing the accuracy of each image, the highest values were observed for the Manual and Otsu method when preceded by the ED index, which resulted in 95.9% of accuracy for both methods. According to Nejati et al. [23], the ED method is based on the search for homology among plants, where after obtaining the spectral energy of plant content; its similarity is verified through the Euclidean distance measurement. Fig. 2 shows examples of resulting images from the proposed segmentation algorithms.
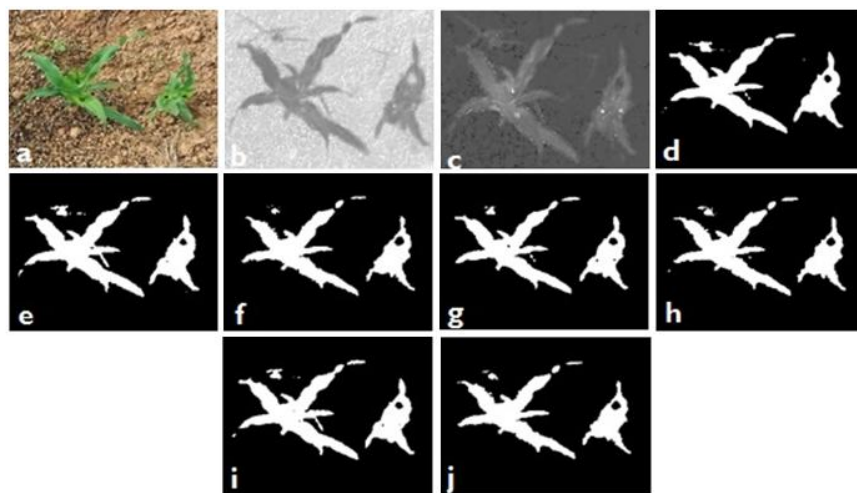

Fig. 2. Images processed by the proposed segmentation algorithms. (a) RGB image, (b) Euclidean distance, (c) ExG index, (d) K-means, (e) Bayes with ED, (f) Bayes with ExG, (g) Manual with ED, (h) Manual with ExG, (i) Otsu with ED, and (j) Otsu with ED

Table 2. Accuracy results from the proposed segmentation algorithms

Methods	Accuracy (%)				
	Max	Min	SD	CV	Mean
Otsu + ED	95.9	32.0	25.65	33.28	77.1
Otsu + ExG	90.9	61.6	9.09	11.33	80.3
Manual + ED	95.9	32.0	23.43	31.99	73.3
Manual ExG	93.5	55.9	13.05	17.12	76.2
Bayes + ED	93.7	22.5	26.15	34.72	75.3
Bayes + ExG	90.9	61.6	16.11	21.19	76.0

Max: maximum; Min: minimal; SD: Standard deviation; CV: coefficient of variation. ED: Euclidean distance;
ExG: Excess of green

In order to determine the most accurate method, the data set was submitted to the Student t-test at 5% significance level. Results from the ANOVA showed that statistically, there was no difference in performance among the proposed methods when compared to each other. Although, the highest CV values were obtained through Bayes (34.72%), and Otsu methods (33.28%), when preceded by the ED index as it is shown in Table 2.

These results can be justified by the adverse illumination conditions during the image acquisition period, which resulted in erroneous segmentation due to shaded areas in images. Thus, the Otsu, manual, and Bayes segmentation methods presented satisfactory accuracy (up to 73.3%) for separating crop canopy from the soil when preceded by the ExG and ED indices. Even though a satisfying performance has been achieved, there are still factors, such as the lighting conditions, plant shading and complex background that are challenges to the success of segmentation.

Thus, the application of low-cost consumer cameras for process control as an element of precision farming could save fertilizer, pesticides, machine time, and labor force. Although research activities on this topic have increased over the years, high camera prices still reflect on low adaptation to applications in all fields of agriculture. Smart cameras adapted to agricultural applications can overcome this drawback.

4. CONCLUSION

The webcam sensor was capable of detecting the effect of nitrogen doses over the Batatais grass through different NDVI values at 7 and 21 days after N application. Regarding the use of webcam images in agricultural applications through thresholding methods, it was possible to observe that the segmentation process over RGB images becomes challenging due to non-uniform illumination conditions, and complex image background. Thus, the use of thresholding methods, such as Otsu, Manual, and Bayes when previously processed by the ExG and ED indices can satisfactorily separate the crop canopy from the soil. As a recommendation for future studies, both images (NIR and RGB) can be used to calculate vegetation indexes to perform studies on phenology or plant's nutritional status. Also, the RGB images can be processed using segmentation algorithms to quantify plant diseases or leaves damaged by pests in crops.

COMPETING INTERESTS

Authors have declared that no competing interests exist.

REFERENCES

1. Yang C, Westbrook JK, Suh CPC, Martin DE, Hoffmann WC, Lan Y, Goolsby JA. An airborne multispectral imaging system based on two consumer-grade cameras for agricultural remote sensing. Remote Sensing. 2014;6(6):5257-5278.
    DOI:https://doi.org/10.3390/rs6065257.

2. Lebourgeois V, Bégué A, Labbé S, Mallavan B, Prévot L, Roux B. Can commercial digital cameras be used as multispectral sensors? A crop monitoring test. Sensors. 2008;8(11):7300-7322.
    DOI:https://doi.org/10.3390/s8117300.

3. Sonnentag O, Hufkens, K, Teshera-Sterne C, Young AM, Friedl M, Braswell BH, Milliman T, O'keefe J, Richardson AD. Digital repeat photography for phenological research in forest ecosystems. Agricultural and Forest Meteorology. 2012;152(1):159–177.

DOI:https://doi.org/10.1016/j.agrformet.201 1.09.009.

4. Rouse JW, Haas Jr. RH, Schell JA, & Deering DW. Monitoring vegetation systems in the Great Plains with ERTS, NASA SP-351. Third ERTS-1 Symposium, 1974;1:309–317, NASA, Washington, DC.

5. Nijland W, De Jong R, De Jong SM, Wulder MA, Bater CW, Coops NC. Monitoring plant condition and phenology using infrared sensitive consumer grade digital cameras. Agricultural and Forest Meteorology. 2014;184(1):98-106.
DOI:https://doi.org/10.1016/j.agrformet.201 3.09.007.

6. Rabatel G, Gorretta N, Labbé N. Getting simultaneous red and near-infrared band data from a single digital camera for plant monitoring applications: Theoretical and practical study. Biosystems Engineering. 2014;117(1):2–14.
DOI:https://doi.org/10.1016/j.biosystemse ng.2013.06.008.

7. Jia B, He H, Ma F, Diao M, Jiang G, Zheng Z, Cui J, Fan H. Use of a digital camera to monitor the growth and nitrogen status of cotton. The Scientific World Journal. 2014;1:1-12.
DOI:http://sci-hub.tw/10.1155/2014/602647.

8. Castro AI, Ehsani R, Ploetz RC, Crane JH, Buchanon S. Detection of laurel wilt disease in avocado using low altitude aerial imaging. PloS one. 2015;10(4):1-13.
DOI:https://doi.org/10.1371/journal.pone.0 124642.

9. Stroppiana D, Migliazzi M, Chiarabini V, Crema A, Musanti M, Franchino C, Villa P.. Rice yield estimation using multispectral data from UAV: A preliminary experiment in northern Italy. In Geoscience and Remote Sensing Symposium (IGARSS), IEEE International. 2015;4664-4667.
DOI:https://doi.org/10.1109/IGARSS.2015. 7326869.

10. Romeo J, Guerrero JM, Montalvo M, Emmi L, Guijarro M, Gonzalez-De-Santos P, Pajares G.. Camera sensor arrangement for crop/weed detection accuracy in agronomic images. Sensors. 2013;13(4): 4348-4366.
DOI:http://sci-hub.tw/10.3390%2Fs130404348.

11. Montalvo M, Guerrero JM, Romeo J, Emmi L, Guijarro M, Pajares G. Automatic expert system for weeds/crops identification in images from maize fields. Expert Systems with Applications. 2013;40(1):75-82.
DOI:https://doi.org/10.1016/j.eswa.2012.07 .034.

12. Torres-Sánchez J, López-Granados F, Peña M. An automatic object-based method for optimal thresholding in UAV images: Application for vegetation detection in herbaceous crops. Computers and Electronics in Agriculture. 2015;114(6):43-52.
DOI:https://doi.org/10.1016/j.compag.201 5.03.019.

13. Sakamoto T, Shibayama M, Kimura A, Takada E. Assessment of digital camera-derived vegetation indices in quantitative monitoring of seasonal rice growth. ISPRS Journal of Photogrammetry and Remote Sensing. 2011;66(6):872-882.
DOI:https://doi.org/10.1016/j.isprsjprs.2011 .08.005.

14. Caturegli L, Corniglia M, Gaetani M, Grossi N, Magni S, Migliazzi M, Angelini L, Mazzoncini, M, Silvestri N, Fontanelli M, Raffaelli M, Peruzzi A, Volterrani M. Unmanned aerial vehicle to estimate nitrogen status of turfgrasses. PloS one. 2016;11(6):1-13.
DOI:https://journals.plos.org/plosone/article ?id=10.1371/journal.pone.0158268.

15. Levin N, Ben-Dor E, & Singer A. 2005. A digital camera as a tool to measure colour indices and related properties of sandy soils in semiarid environments. International Journal of Remote Sensing, 26(24), 5475–5492. DOI: https://doi.org/10.1080/0143116050009944 4.

16. Vesali F, Omid M, Kaleita A, & Mobli H. 2015. Development of an android app to estimate chlorophyll content of corn leaves based on contact imaging. Computers and Electronics in Agriculture, 116, 211-220. DOI: https://doi.org/10.1016/j.compag.2015.06.0 12.

17. Aureliano Netto AF, Martins RN, Aquino de Souza GS, Araujo GDM, Hatum de Almeida SL, Capelini VA. Segmentation of RGB images using different vegetation indices and thresholding methods. NATIVA. 2018;6(4):389-394.
DOI:http://dx.doi.org/10.31413/nativa.v6i4. 5405

18. Micha DN, Penello G, Kawabata RMS, & Camarott T. 2011. Vendo o invisível.

Experimentos de visualização do infravermelho feitos com materiais simples e de baixo custo. Revista Brasileira de Ensino de Física. 2011;33(1):1501. DOI:http://sci-hub.tw/10.1590/S1806-11172011000100015.

19. Minolta Camera Co. Ltd. Chlorophyll meter SPAD-502 Instructional Manual. Minolta, Osaka, Japan. 1989;22.

20. Silva FAS, Azevedo CAV. The assistat software version 7.7 and its use in the analysis of experimental data. African Journal of Agricultural Research. 2016;11(39):3733-3740. DOI:https://doi.org/10.5897/AJAR2016.11522.

21. Otsu N. A threshold selection method from gray-level histogram. IEEE Transactions on System Man Cybernetics. 1979;9(1):62-66. DOI:https://doi.org/10.1109/TSMC.1979.4310076.

22. Gonzales RC, Woods RE. Digital image processing (vol.2). Addison-Wesley Publishing Company; 1992.

23. Nejati H, Azimifar Z, Zamani M. Using fast fourier transform for weed detection in corn fields. In Systems, Man and Cybernetics. IEEE International Conference. 2008;1215-1219. DOI:https://doi.org/10.1109/ICSMC.2008.4811448.

24. Woebbecke DM, Meyer GE, Von Garden K, Mortensen DA. Color indices for weed identification under various soil, residue and lighting conditions. Transactions of the ASAE. 1995;38:259–269. DOI:http://sci-hub.tw/10.13031/2013.27838.

25. Dass R, Priyanka, Devi S. Image segmentation techniques. International Journal of Electronics & Communication Technology. 2012;3(1):1-5.

26. Coy A, Rankine D, Taylor M, Nielsen DC, Cohen J. Increasing the accuracy and automation of fractional vegetation cover estimation from digital photographs. Remote Sensing. 2016;8(7):474-488. DOI:https://doi.org/10.3390/rs8070474.

27. Petach AR, Toomey M, Aubrecht DM, Richardson AD. Monitoring vegetation phenology using an infrared-enabled security camera. Agricultural and Forest Meteorology. 2014;195(9):143–151. DOI:https://doi.org/10.1016/j.agrformet.2014.05.008.

28. Baesso MM, de Carvalho Pinto FDA, de Queiroz D, Santos NT, de Souza Carneiro JE. Avaliação da deficiência de nitrogênio no feijoeiro usando um medidor portátil de clorofila. Engenharia na Agricultura. 2013;21(2):122-128. DOI:https://doi.org/10.13083/reveng.v21i2.318.

29. Ryu Y, Lee G, Jeon S, Song Y, Kimm H. Monitoring multi-layer canopy spring phenology of temperate deciduous and evergreen forests using low-cost spectral sensors. Remote Sensing of Environment. 2014;149(6):227–238. DOI:http://sci-hub.tw/10.1016%2Fj.rse.2014.04.015.

30. Ryu Y, Baldocchi DD, Verfaillie J, Ma S, Falk M, Ruiz-Mercado I, Hehn T, Sonnentag O. Testing the performance of a novel spectral reflectance sensor, built with light emitting diodes (LEDs), to monitor ecosystem metabolism, structure and function. Agricultural and Forest Meteorology. 2010;150(12):1597–1606. DOI:https://doi.org/10.1016/j.agrformet.2010.08.009.

31. Hamuda E, Glavin M, Jones E. A survey of image processing techniques for plant extraction and segmentation in the field. Computers and Electronics in Agriculture. 2016;125(7):184-199. DOI:https://doi.org/10.1016/j.compag.2016.04.024.

32. Bai X, Cao Z, Wang Y, Yu Z, Hu Z, Zhang X, Li C. Vegetation segmentation robust to illumination variations based on clustering and morphology modelling. Biosystems Engineering. 2014;125(9):80-97. DOI:https://doi.org/10.1016/j.biosystemseng.2014.06.015.

Peer-review history:
The peer review history for this paper can be accessed here:
http://www.sdiarticle3.com/review-history/47692